



Optimization of light propagation in Amplified Multimode Optical Fibers

CISNEROS Hugo
September 2016 - January 2017
Paris

Supervised by Tom Sperber
and Sylvain Gigan

Laboratoire Kastler-Brossel
Département de Physique Ecole Normale Supérieure
24 rue Lhomond
75005 Paris, France

Acknowledgements

I would like to express my gratitude towards all the people who helped me complete this project and write this report. A special gratitude I give to my supervisors Tom Sperber and Sylvain Gigan who helped me from the beginning and who gave me such attention and time. My thanks and appreciations also go to my colleague from LKB at Lhomond and Jussieu in helping me and answering my questions and to people who willingly helped me out with their abilities.

Contents

| | |
|--|-----------|
| Introduction | 4 |
| 1 Theory of optical fibers | 5 |
| 1.1 Weakly-guiding step-index fibers | 5 |
| 1.1.1 General description | 5 |
| 1.1.2 Field propagation in a fiber | 6 |
| 1.1.3 Eigenvalue equations for the LP modes | 9 |
| 1.1.4 LP modes characteristics | 12 |
| 1.2 Transmission Matrices and Multimode Fibers | 15 |
| 1.2.1 Transmission Matrices | 16 |
| 1.2.2 Modal Transmission Matrices and MMFs | 17 |
| 2 Simulating the propagation of light through a MMF | 18 |
| 2.1 The model | 18 |
| 2.1.1 Incoming beam in a MMF | 18 |
| 2.1.2 Rare-earth amplified fiber | 19 |
| 2.2 The simulation and its challenges | 21 |
| 3 Results of the simulations | 23 |
| 3.1 Maximizing an off diagonal element | 23 |
| 3.2 Minimizing a diagonal element | 25 |
| 3.3 Intermodal coupling | 27 |
| A Appendix | 32 |

Introduction

This report aims to present and explain the work I carried out during my part time research internship between September 2016 and January 2017. I worked with PhD candidate Tom Sperber in Sylvain Gigan's group Optical imaging in biological and complex media at Kastler-Brossel lab (LKB) of ENS. The group studies mainly optical imaging through scattering media with state-of-the art techniques such as wavefront shaping and transmission matrix measurement [10], [3].

Multimode Fibers are optical fibers with several possible guided modes of light transmission. When light propagates through a Multimode Fiber (MMF), it couples with all the possible guided modes of the fiber. Although they are not a scattering medium, the modal dispersion phenomenon makes it difficult to practically understand the signal's behavior. Because of the slightly different propagation constant of each mode, a dephasing appears between the mode components when the signal beam propagates and after a certain distance it becomes deteriorated. For long scientists have believed that the mixing inside the fiber was too complex to understand, but the apparent randomness is only due to multiple dephasing between every modes and all the mode combinations are linear. Transmission matrices measurements - the matrix representing the mapping between input and output modes - along with wavefront shaping - fine and dynamic modulation of the light field wavefront with spatial light modulators (SLM) - have enabled physicists to entirely characterize light transmission in MMFs. With a fiber's transmission matrix, one can know which modes at the input correspond to a particular output and use it to perform imaging or focusing for instance.

Multimode Fiber Amplifiers (MMFA) are MMF made of amplifying material that can be excited by a pump beam. Because a pump beam propagates similarly to a signal beam, as a superposition of guided modes of the fiber, the modal composition of the pump is expected to mix non uniformly and have an influence on the Transmission Matrix of the fiber. However, this influence is likely to be complex and hard to predict . Being able to control this effect of the pump beam on the Transmission Matrix would allow to cope with nonlinear effects that arise when using MMFs with high optical intensities or to improve telecommunication applications of MMFs.

So far, the link between the modal composition of an amplifying pump and the transmission matrix of a fiber hasn't been investigated in depth. The strong influence of perturbations of the pump on the transmission matrix has been observed but it is not certain if this influence can be controlled and targeted to some specific matrix configuration and if so, in what extent.

During my internship, I developed a numerical optimization tool that theoretically

demonstrates significant maximization of some specific elements of the transmission matrix, that is to say the amount of energy a specific mode will receive when inputting another given mode in the MMFA. The simulation is able to find an optimal pump configuration for any given target transmission matrix. Minimization and near extinction of the self-amplification component of some modes has been observed after optimization, raising interesting questions about the possibility of controlling the pump to achieve specific effects on the transmission matrix.

The report begins with a review of the theory of optical fibers and Multimode fibers, and of the relation between the modal behavior of light in MMFs and their Transmission Matrices. Then, the model used for calculating the Transmission Matrix of a Multimode Fiber Amplifier is described and its implementation and the challenges the simulation posed are exposed. Finally, the results provided by the optimization scheme are analyzed.

Theory of optical fibers

1.1 Weakly-guiding step-index fibers

1.1.1 General description

Structure of an optical fiber

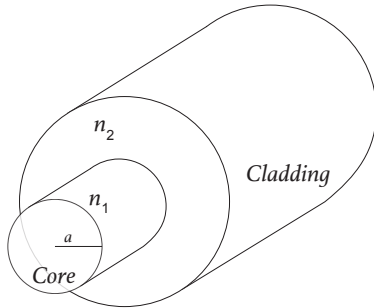


Figure 1.1 – Description of the structure of an optical fiber

A single step-index optical fiber consists of two homogeneous concentric dielectrics as shown on Figure 1.1. The inner dielectric, referred to as the *core*, fills the region $r < a$ and is of refractive index n_1 . The cladding is the region corresponding to $r > a$, of refractive index n_2 , with $n_2 < n_1$; it is considered of infinite outer radius for purpose of analysis (in practice, the ratio between the two diameters depends on the wavelength application but falls between 1% and 0.2%). Among the key structural parameters of a fiber are the core radius a and the *normalized index difference* Δ , defined as follows :

$$\Delta = \frac{n_1^2 - n_2^2}{2n_1^2} \quad (1.1)$$

The *numerical aperture (NA)* is also an important parameter of an optical fiber. It is defined as the sine of the maximum angle of an incident light ray which has been totally confined into the fiber. The expression of this quantity can be found by geometrical means, using Snell-Descartes' law on a 2-D restriction of the problem as described Figure 1.2. On the figure, a ray with an incidence angle of θ_{NA} is refracted at the interface air/fiber and is reflected at the interface between the core and the cladding if and only if its incidence angle is greater than θ_c , with $\sin \theta_c = \frac{n_2}{n_1}$. Therefore, we find that

$$NA = \sin \theta_{NA} = \frac{1}{n_0} \sqrt{n_1^2 - n_2^2} = \frac{n_1}{n_0} \sqrt{2\Delta} \quad (1.2)$$

The weakly-guiding approximation

In further analysis, we will consider that the fibers satisfy the *weakly-guiding approximation*. This approximation states that the two refractive indexes n_1 and n_2 are very close in value from each other, that is to say $\Delta = \frac{n_1^2 - n_2^2}{2n_1^2} \ll 1$.

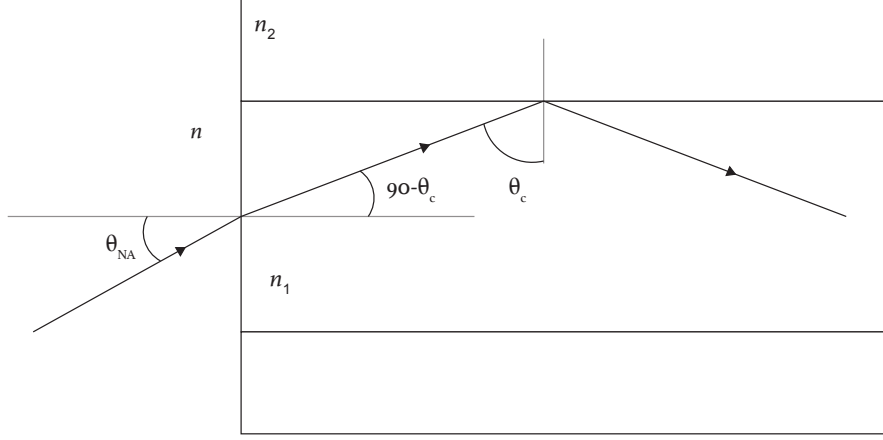


Figure 1.2 – Ray propagation for an input of incidence angle θ_{NA} in a 2-D restriction of the fiber

This approximation is almost always true for commercial glass fibers, and it yields a relatively small numerical aperture of the device.

For practical reasons further explained, optical fibers are classified into single-mode fibers, which have values of Δ typically around 0.2% and multimode fibers with Δ s of the order of 1%.

In all the following, only step-index fibers will be studied. It has in many instances been replaced by more specific and complicated profiles. Alternative profiles can have a larger acceptable bandwidth, less dispersion for some wavelengths and enable to better control polarization inside the fiber. Nonetheless, modes inside those fibers have the same characteristics and general behavior, hence the focus on step-index fibers.

1.1.2 Field propagation in a fiber

Wave Equations for LP modes

Because of the reasoning based on a slab waveguide, explained in [2], the field solutions are considered as being linearly polarized in the fiber transverse plane (the electric field is designated as having an x polarization and the magnetic field as having a y polarization). It can be shown that the magnitude of the z components of the field are lower than those of the transverse plane by a factor of the order of $\sqrt{\Delta}$ and because of the weakly-guiding approximation, we will neglect this part of the field. Therefore, the fields components are written

$$\mathbf{E} = E_x(r, \varphi, z)\hat{\mathbf{a}}_x = E_{x0}(r, \varphi)e^{-i\beta z}\hat{\mathbf{a}}_x \quad (1.3)$$

$$\mathbf{H} = H_y(r, \varphi, z)\hat{\mathbf{a}}_y = H_{y0}(r, \varphi)e^{-i\beta z}\hat{\mathbf{a}}_y \quad (1.4)$$

Rectangular components are assumed for the field and the wave equation is separable into x and y components, and we have

$$\nabla_t^2 E_{x,core} + (n_1^2 k_0^2 - \beta^2) E_{x,core} = 0, \quad r \leq a \quad (1.5)$$

$$\nabla_t^2 E_{x,clad} + (n_2^2 k_0^2 - \beta^2) E_{x,clad} = 0, \quad r \geq a \quad (1.6)$$

Where $k_0 = 2\pi/\lambda_0$ is the wave number in free space. The *propagation constant* β of any mode is always limited in the interval $n_1 k_0 \geq \beta \geq n_2 k_0$ [2]. If we define the parameters

$$u = a(k_0^2 n_1^2 - \beta^2)^{\frac{1}{2}} \quad (1.7)$$

$$w = a(\beta^2 - k_0^2 n_2^2)^{\frac{1}{2}}, \quad (1.8)$$

we find for the wave equation in both regions,

$$\frac{\partial^2 E_{x,core}}{\partial r^2} + \frac{1}{r} \frac{\partial E_{x,core}}{\partial r} + \frac{1}{r^2} \frac{\partial^2 E_{x,core}}{\partial \varphi^2} + \frac{u^2}{a^2} E_{x,clad} = 0 \quad (1.9)$$

$$\frac{\partial^2 E_{x,clad}}{\partial r^2} + \frac{1}{r} \frac{\partial E_{x,clad}}{\partial r} + \frac{1}{r^2} \frac{\partial^2 E_{x,clad}}{\partial \varphi^2} - \frac{w^2}{a^2} E_{x,clad} = 0 \quad (1.10)$$

Those equations are easily transposable to the magnetic field and the parameter v , defined as

$$v^2 = u^2 + w^2, \quad (1.11)$$

$$v = ak_0(n_1^2 - n_2^2)^{\frac{1}{2}} \quad (1.12)$$

can be interpreted as a normalized frequency. We assume the solution to be a discrete series of modes with separate dependencies on r, φ and z in product form. The separate dependencies on z correspond to separate propagation constants. Each of those modes must itself be solution to (1.10):

$$E_x = \sum_{i=1}^n R_i(r) \Phi_i(\varphi) e^{-j\beta_i z} \quad (1.13)$$

A single mode can be substituted into (1.10) to obtain the following equations

$$\frac{r^2}{R} \frac{d^2 R}{dr^2} + \frac{r}{R} \frac{dR}{dr} + r^2 \frac{u^2}{a^2} = -\frac{1}{\Phi} \frac{d^2 \Phi}{d\varphi^2} \quad (1.14)$$

in the core and,

$$\frac{r^2}{R} \frac{d^2 R}{dr^2} + \frac{r}{R} \frac{dR}{dr} - r^2 \frac{w^2}{a^2} = -\frac{1}{\Phi} \frac{d^2 \Phi}{d\varphi^2} \quad (1.15)$$

in the cladding.

The left hand-side of both equations depends only on r and their right hand-side depends only on φ . Because r and φ vary independently, each side of (1.14) and (1.15) must be equal to a constant, defined as ℓ^2 . We can separate the two sides and write for example in the core :

$$\frac{d^2 \Phi}{d\varphi^2} + \ell^2 \Phi = 0 \quad (1.16)$$

$$\frac{d^2 R}{dr^2} + \frac{1}{R} \frac{dR}{dr} + \left[\frac{u^2}{a^2} - \frac{\ell^2}{r^2} \right] R = 0 \quad (1.17)$$

Solutions of the wave equations

Equation (1.16) can readily be solved and it yields :

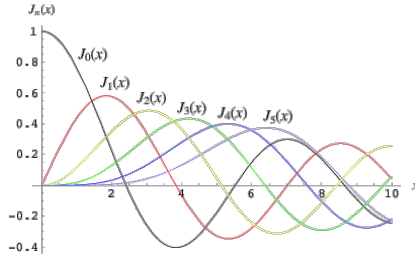
$$\Phi(\varphi) = \begin{cases} \cos(\ell\varphi + \alpha) \\ \sin(\ell\varphi + \alpha) \end{cases} \quad (1.18)$$

where α is a constant. Because the field must be self-consistent over a 2π rotation of φ , we have $2\pi\ell = 2k\pi$, with k integer, and ℓ must be an integer. For linearly polarized modes, the parameter ℓ is called the angular (or azimuthal) mode number.

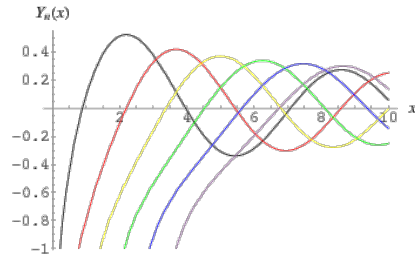
Equation (1.17) is a form of Bessel's equation. Its solution in term of Bessel functions is [15],[14]

$$R(r) = \begin{cases} AJ_\ell\left(\frac{ur}{a}\right) + A'Y_\ell\left(\frac{ur}{a}\right), & r \leq a \\ BK_\ell\left(\frac{wr}{a}\right) + B'I_\ell\left(\frac{wr}{a}\right), & r > a \end{cases} \quad (1.19)$$

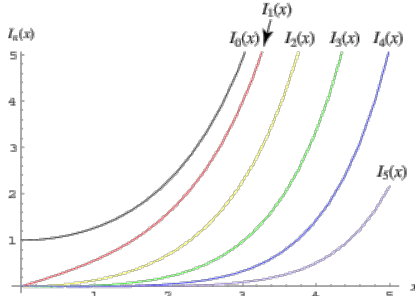
where J_ℓ and Y_ℓ are Bessel functions of the first and second kinds of order ℓ , and K_ℓ and I_ℓ are modified Bessel functions of the first and second kind of order ℓ , which apply because of the factor $-\frac{w^2}{a^2}$ in (1.15). The behavior of the four functions is depicted on Figure 1.3.



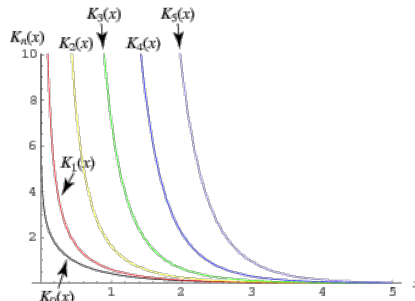
(a) Bessel function of the first kind



(b) Bessel function of the second kind



(c) Modified Bessel function of the first kind



(d) Modified Bessel function of the second kind

Figure 1.3 – Behavior of the four Bessel functions for several orders

Because the basic properties of a guided mode in a waveguide still apply in our case, we expect the solution to be oscillatory, exhibiting no singularities in the core and to monotonically decrease in the cladding. Therefore, A' and B' must be equal to zero. Then, using the $\cos(\varphi\ell)$ dependency in (1.16) and setting $\alpha = 0$, we obtain the

complete solution for E_x :

$$E_x(r, \varphi, z) = \begin{cases} AJ_\ell\left(\frac{ur}{a}\right) \cos(\ell\varphi) \exp(-i\beta z), & r \leq a \\ BK_\ell\left(\frac{wr}{a}\right) \cos(\ell\varphi) \exp(-i\beta z), & r > a \end{cases} \quad (1.20)$$

Similarly, we can solve the wave equation (1.4) for the magnetic field, leading to :

$$H_y(r, \varphi, z) = \begin{cases} CJ_\ell\left(\frac{ur}{a}\right) \cos(\ell\varphi) \exp(-i\beta z), & r \leq a \\ DK_\ell\left(\frac{wr}{a}\right) \cos(\ell\varphi) \exp(-i\beta z), & r > a \end{cases} \quad (1.21)$$

With the quasi plane wave approximation introduced at the beginning of the analysis, we also have

$$A \approx \eta B \quad \text{and} \quad C \approx \eta D \quad (1.22)$$

Boundary conditions

Applying the boundary conditions for the field at the core-cladding interface, we can get an expression of the coefficients A , B and C , D in terms of a single quantity. For the electric fields, the boundary conditions are expressed as follow

$$E_{\varphi 1}|_{r=a} = E_{\varphi 2}|_{r=a} \quad (1.23)$$

$$n_1^2 E_{r1}|_{r=a} = n_2^2 E_{r2}|_{r=a} \quad (1.24)$$

The weakly guiding approximation yields $n_1 \approx n_2$. And because both normal and tangential components of E are continuous across the interface, setting $A = E_0$ and using (1.20) we have the final expression for the electric field

$$E_x(r, \varphi, z) = \begin{cases} E_0 J_\ell\left(\frac{ur}{a}\right) \cos(\ell\varphi) \exp(-i\beta z), & r \leq a \\ E_0 [J_\ell(u)/K_\ell(w)] K_\ell\left(\frac{wr}{a}\right) \cos(\ell\varphi) \exp(-i\beta z), & r > a \end{cases} \quad (1.25)$$

Equation (1.25) is the general electric field for mode $\text{LP}_{\ell m}$. The two subscripts are the angular mode number ℓ and the radial mode number m . From the equation (1.25), it is easy to understand how ℓ is related to the number of variations around a circle in the transverse plane of the fiber. The number m doesn't appear explicitly in (1.25) because it specifies allowed range of u as explained later. The larger m is, the larger u will be, which implies a greater number of oscillations of the function $J_\ell(ur/a)$. A more specific interpretation of the mode numbers will be given further, along with field profiles.

1.1.3 Eigenvalue equations for the LP modes

To determine the conditions under which a guided mode can occur (core radius, index difference between core and cladding, etc.), we need to find the solution to the eigenvalue equation for the given parameters. This equation is derived using the continuity

condition of the z component of the fields at $r = a$ and is precisely detailed in [2]. It is written

$$u \frac{J_{\ell-1}(u)}{J_\ell(u)} = -w \frac{K_{\ell-1}(w)}{K_\ell(w)} \quad (1.26)$$

Solving this equation yields phase constants and field profiles [using (1.25)] for each mode that can propagate in a fiber with any choice of dimensions, operating wavelengths and materials. One way to solve it gives a good understanding of the repartition of the roots and is interesting when trying to find all the possible modes in a given fiber.

Graphical Solution Method

This method consist in an analysis of the functions constituting the two sides of (1.26) to find solutions of the eigenvalue equation. The method is illustrated on Figure 1.4 for the case $\ell = 1$ where (1.26) becomes

$$\frac{J_1(u)}{J_0(u)} = -\frac{u}{w} \frac{K_1(w)}{K_0(w)} \quad (1.27)$$

The left hand side of this equation, when plotted as a function of u , resembles a tangent function. As shown in Figure 1.4, to the branches of the function are assigned numbers the correspond to values of m , beginning with $m = 1$. The numbering is done separately on the upper and lower half-planes.

The right hand side of (1.27) is plotted as a function of $u = (v^2 - w^2)^{1/2}$ for $V = 2$, 8 and 11 in Figure 1.4. By setting $w = 0$ we get the upper bound for u before which the solutions of the equation can be found. The same graph is used to exhibit LP_{0m} modes. When setting $\ell = 0$ in (1.26) and using the relations $J_{-1} = -J_1$ and $K_{-1} = K_1$, we obtain

$$\frac{J_1(u)}{J_0(u)} = \frac{w}{u} \frac{K_1(w)}{K_0(w)} \quad (1.28)$$

Some similar plots can be made for LP_{lm} modes for $l \geq 2$. The curves $J_\ell/J_{\ell-1}$ thereby produced fall between some of the curves of Figure 1.4, making the progression of acceptable modes with increasing v somewhat more complicated than the simple alternate case illustrated. It gets more complex as the value of v gets bigger because higher order modes can propagate. We can note the single-mode operation, when only the fundamental mode will be able to propagate, occurs when only the very first branch in Figure 1.4 intersects the other curve. Therefore, the range of values for those operations is $0 < v < 2.405$.

Mode Designation

Mode ordering and designation is determined by their cutoff conditions, that is to say the minimum value of v allowing this mode to propagate. It can directly be found using (1.26) and setting $w = 0$. The cutoff condition obtained is therefore

$$v_c \frac{J_{\ell-1}(v_c)}{J_\ell(v_c)} = 0 \quad (1.29)$$

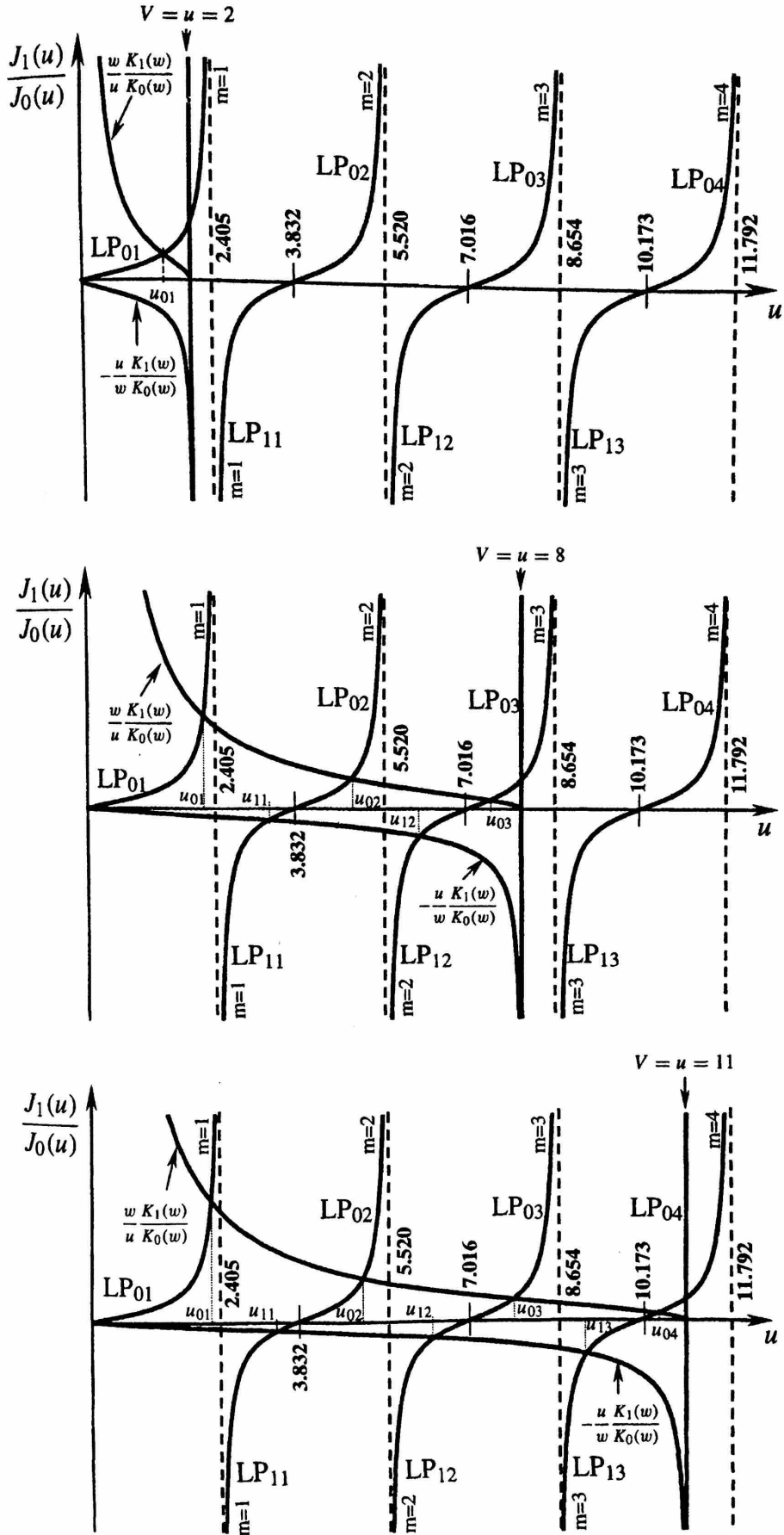


Figure 1.4 – Graphical method illustration for LP_{0m} and LP_{1m}

It is satisfied for all zeros of $J_{\ell-1}$. The case $v_c = 0$ is handled by the approximation of $J_\ell(v)$ valid for small values of v ,

$$J_\ell(v) \approx \frac{1}{\ell!} \left(\frac{v}{2}\right)^\ell \quad (1.30)$$

Equation (1.29) becomes

$$\frac{\ell v_c (v_c/2)^{\ell-1}}{(v_c/2)^\ell} = 2\ell \quad (1.31)$$

which is zero only when $\ell = 0$ and therefore uniquely applies to LP₀₁ mode with $v_c = 0$. When $v_c \neq 0$, (1.29) becomes the simple expression

$$J_{\ell-1}(v_c) = 0 \quad (1.32)$$

Cutoff conditions are identified as zeros of Bessel functions with a restriction for $v_c = 0$. The ordering of the modes progresses when finding the zeros of Bessel function and LP _{ℓm} is associated with the m^{th} zeros of $J_{\ell-1}$. When fibers parameters are given, all the modes that can propagate can be deduced by this list of zeros.

1.1.4 LP modes characteristics

To visualize how LP modes behave and are ordered, we plot several intensity profiles for different propagating LP modes in a given fiber. The intensity is found by evaluating the time average of the Poynting vector, which is in the case of the quasi plane wave approximation

$$| \langle \mathbf{S} \rangle | = \frac{1}{2} \operatorname{Re}(E_x H_y^*) = \frac{1}{2\eta} |E_x|^2 \quad (1.33)$$

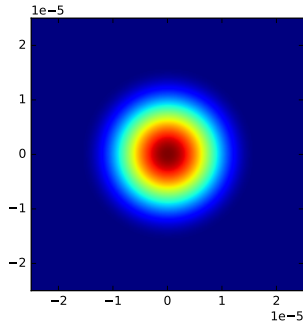
Defining I_0 the peak intensity, the intensity function for a LP mode is written

$$I_{lm} = \begin{cases} I_0 J_\ell^2 \left(\frac{ur}{a} \right) \cos^2(\ell\varphi), & r \leq a \\ I_0 [J_\ell(u)/K_\ell(w)]^2 K_\ell^2 \left(\frac{wr}{a} \right) \cos^2(\ell\varphi), & r > a \end{cases} \quad (1.34)$$

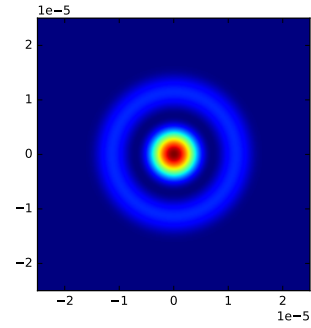
Figure 1.5 shows intensity plots for eight LP modes, calculated from (1.34), along with the label of the mode. The significance of ℓ and m now becomes apparent. ℓ is half the number of maxima that occur in the intensity over a 2π rotation of φ and m is the number of maxima encountered along a radial line between zero and infinity. For $\ell = 0$, two polarization state can occur : one for each polarization axis inside the fiber. For $\ell \geq 1$, each mode has 4 different polarization state, two because of the two solutions found in (1.16) and two others for the polarization axis of the fiber. In the model studied further, only one polarization axis is taken into account for the simulations.

Computing the parameters

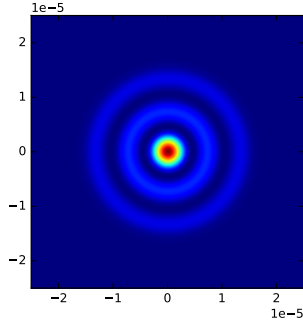
The resolution of (1.26) yields all the necessary parameters for simulating light propagation in a given fiber and a complete description of LP modes. More straightforward methods [4] enable to solve approximately (1.26) and obtain simple expressions of u , β , etc. as functions of the fiber parameters.



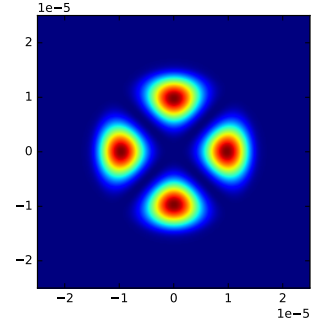
(a) LP₀₁



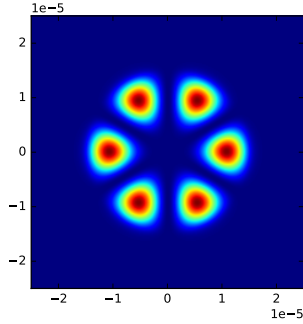
(b) LP₀₂



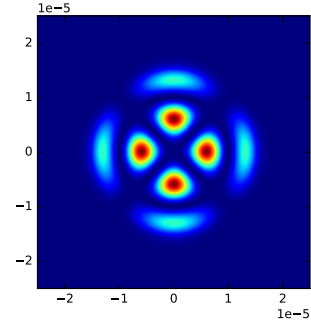
(c) LP₀₃



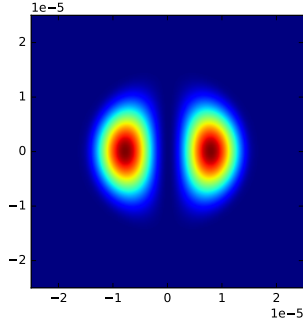
(d) LP₂₁



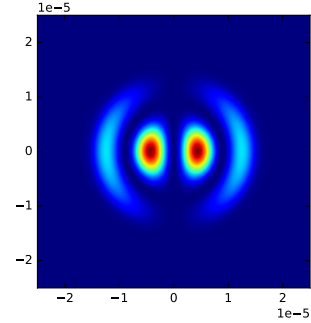
(e) LP₃₁



(f) LP₂₂



(g) LP₁₁



(h) LP₁₂

Figure 1.5 – Several modes in a fiber of core radius $15\mu m$ with $v = 12$

First, the characteristic equation (1.26) is differentiated with respect to v , yielding the new characteristic equation

$$\frac{du}{dv} = \frac{u}{v}(1 - \kappa_\ell(w)) \quad (1.35)$$

where

$$\kappa_\ell(w) = \frac{K_{\ell^2}(w)}{K_{\ell-1}(w)K_{\ell+1}(w)} \approx 1 - (w^2 + l^2 + 1)^{-1/2} \quad (1.36)$$

Since u always stays in the narrow region between two successive roots of adjacent Bessel functions, the following approximation where u is replaced by u_c , is valid for all modes except LP₀₁ (its mode parameters u , v and w all approach zero simultaneously):

$$w \approx (v^2 - u_c^2)^{1/2} \quad (1.37)$$

Then, solving (1.35) yields

$$u(v) = u_c \frac{\exp(\arcsin(s/u_c) - \arcsin(s/v))}{s} \quad (1.38)$$

with

$$s = (u_c^2 - l^2 - 1)^{1/2} \quad (1.39)$$

from [4] we get the expression of u as a function of v for LP₀₁

$$u(v) = v \frac{1 + \sqrt{2}}{1 + (4 + v^4)^{1/4}} \quad (1.40)$$

This is an expression of u as a function of the fiber parameters and mode characteristics only. It enables to compute the propagation constant β for a given mode.

We can also plot $b = 1 - u^2/v^2 = (\beta^2/k_0^2 - n_2^2)/(n_1^2 - n_2^2)$, the normalized propagation parameter as a function of the normalized frequency v as done in [4]. The plot is reproduced Figure 1.6 where the number on each curve represents the mode designation as defined in 1.1.3.

We can notice that as expected, the relation $n_1 k_0 \leq \beta \leq n_2 k_0$ is satisfied. Every propagation constant of the LP modes is slightly different from the others and is found in the tiny space between the previous and the next mode's propagation constants.

Those differences in propagation speed lead to the modal dispersion phenomenon in multimode fibers. Every mode component of the field acquires a dephasing when propagating and a signal progressively gets very deteriorated. Table 1.1 shows u , β and the *effective refractive index*, which is defined as $n_{eff} = \beta/k_0$ and represents the uniform refractive index a mode "sees". As for the propagation constants, the effective refractive indexes are all slightly different. To quantify the impact of this difference, we can take a look at the *dephasing length*, or the length after which two modes are dephased of more than 2π radians and could therefore be dephased of any multiple of 2π plus the current observed dephasing. The expression of the dephasing length for several modes is :

$$DL = \min_{\beta_1 \neq \beta_2 \in B} \left| \frac{2\pi}{\beta_1 - \beta_2} \right| \quad (1.41)$$

where B is the set of all the propagation constants of the propagating modes.

For the modes of Table 1.1, the smallest dephasing length is the one between LP₀₁ and LP₁₃ and it is only $306\mu m$. For almost all applications, this number is a lot smaller than the length of fiber needed, hence the need for controlling, predicting or reversing the modal dispersion in order to achieve clean signal transmission.

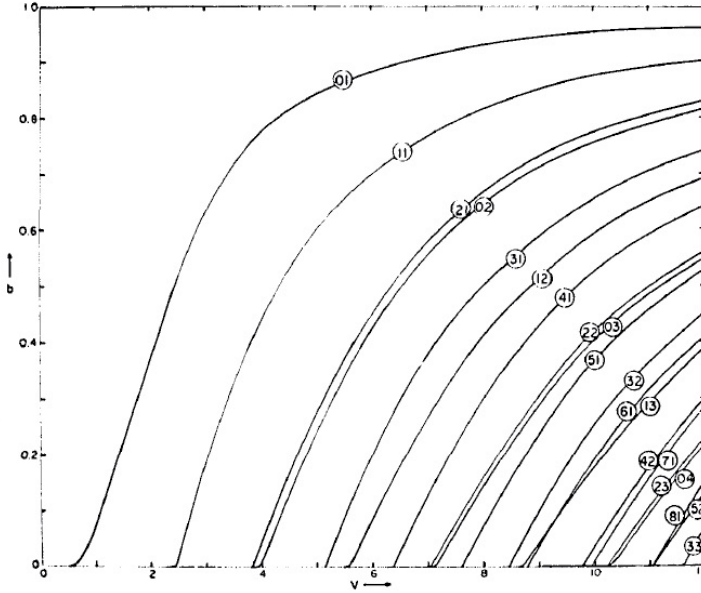


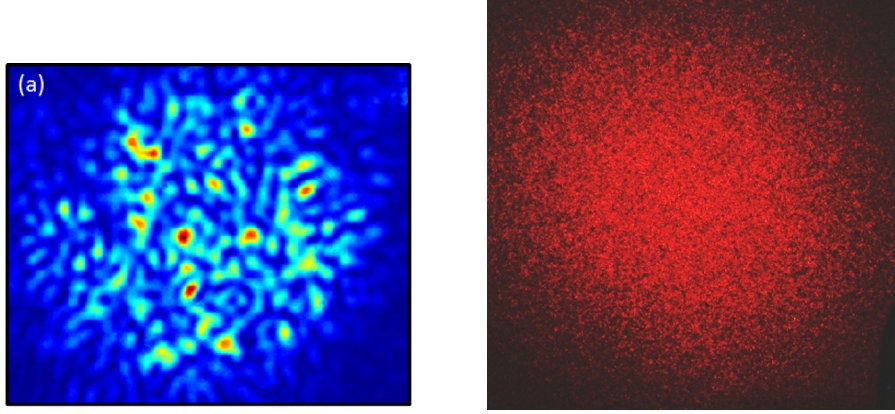
Figure 1.6 – Normalized propagation parameter $b = (\beta^2/k_0^2 - n_2^2)/(n_1^2 - n_2^2)$ as a function of the normalized frequency v . [4]

| Mode designation | u value | Propagation constant β $\times 10^6 m^{-1}$ | Effective refractive index |
|------------------|-----------|--|----------------------------|
| LP ₀₁ | 2.25 | 9.1490 | 1.49980 |
| LP ₁₁ | 3.58 | 9.1471 | 1.49949 |
| LP ₀₂ | 5.16 | 9.1438 | 1.49894 |
| LP ₁₂ | 6.55 | 9.1398 | 1.49829 |
| LP ₀₃ | 8.01 | 9.1344 | 1.49740 |
| LP ₁₃ | 9.47 | 9.1285 | 1.49643 |
| LP ₂₁ | 4.8 | 9.1447 | 1.49908 |
| LP ₃₁ | 5.96 | 9.1416 | 1.49858 |

Table 1.1 – Some mode parameters for a signal in a multimode fiber. The fiber parameters are $a = 15\mu m$, $n_1 = 1.5$, $n_2 = 1.4914$, $v = 14.64$, $NA = 0.16$

1.2 Transmission Matrices and Multimode Fibers

In classical optical systems, propagation of an electromagnetic field is well understood, with diffraction theory for example, as long as multiple scattering doesn't occur. In media for which light is scattered multiple times, light intensity exponentially decreases as the depth increases. All input vectors get mixed up in a seemingly not understandable but still deterministic way. Nonetheless, no information is lost during a multiple scattering event and the speckle pattern (see Figure 1.7) - result of the transmission of coherent light through the medium - is the superposition of the very large number of optical channels light has been transmitted through.



(a) Speckle pattern recorded at $\lambda = 1500\text{nm}$ from the end of a 100m long MMF [11]

(b) Speckle pattern formed when a laser beam was scattered from a plastic surface

Figure 1.7 – Examples of speckle patterns

1.2.1 Transmission Matrices

The transmission matrix of an optical system is defined in [10] as the matrix K of the complex coefficients k_{mn} connecting the optical field in the m^{th} of M output-free mode to the one in the n^{th} of N input-free mode. In other words, it is the matrix representing the linear transformation the medium applies to an optical field, projected at the input on the base of the input-free modes and on the base of the output-free modes at the output.

If we write the projection of the outgoing field on the m^{th} free mode E_m^{out} , we have the relation $E_m^{\text{out}} = \sum_n k_{mn} E_n^{\text{in}}$ for every m where E_n^{in} is the amplitude of the projected field on the n^{th} input free mode. Assuming an incoming field decomposable on the N incoming modes we have :

$$E_{\text{out}} = \sum_m \sum_n k_{mn} E_n^{\text{in}} \quad (1.42)$$

When applied to the canonical basis of the pixels of a CCD and the corresponding discretisation of the input, the TM describes the relation between input and output "pixels" and gives an understanding of the effect of light transmission through it.

Experimentally, spatial light modulators (or SLM) are used to perform so-called *wavefront-shaping* by controlling independently the phase and/or amplitude of every pixel at a particular location in the experimental setup. In practise, although the observed transmission matrix K_{obs} could be inverted to obtain a perfect image transmission and reconstruct a given input from the output speckle, it yields instability in presence of noise. Therefore, the mean square optimized operator (MSO), which minimizes transmission errors [12] is generally used in practise [10],[9].

Knowing the transmission matrix of a medium enables to reconstruct an image by inverting the scattering process [10] or to take advantage of the medium to perform particular effect on a light beam such as focusing by sending the right input into the medium [8], [13].

1.2.2 Modal Transmission Matrices and MMFs

When considering Multimode fibers, an interesting basis for transmission matrices is the one of acceptable LP modes. As explained in section 1.1.3, LP modes are eigenmodes for the fiber, that is to say they only see their phase change when propagating. As guided light in a MMF is always a sum of LP guided modes, an incoming field in a fiber can be represented as a column vector containing the weights of every LP modes in the field. If we denote $\psi_i(x, y, z)$ the i^{th} LP guided mode of the fiber, an input light field can be written

$$E(x, y, z) = \sum_i \alpha_i \psi_i(x, y, z) + \left(E(x, y, z) - \sum_i \alpha_i \psi_i(x, y, z) \right) \quad (1.43)$$

with

$$\alpha_i = \iint E(x', y', z) \psi_i^*(x', y', z) dx' dy' \quad (1.44)$$

And the guided component of the field E is simply represented in the LP guided modes basis by the column vector

$$\alpha = (\alpha_0, \alpha_1, \dots, \alpha_n)^T \quad (1.45)$$

If we know the transmission matrix K of the portion of fiber, the output field can be represented by a column vector $\alpha' = (\alpha'_0, \alpha'_1, \dots, \alpha'_n)^T$ where

$$\alpha' = K\alpha \quad (1.46)$$

Theoretically, the transmission matrix of the fiber in such a basis is a diagonal matrix with the propagation induced phase shift coefficients $e^{-i\beta_i L}$ where L is the length of the fiber.

Experimentally measured MMFs transmission matrices are rarely diagonal but always exhibit mixing between the modes in specific mode groups [8]. These off-diagonal elements can be greatly reduced when improving the input-output alignment for the fiber and reducing its bending.

The transmission matrix obtained on the LP guided modes basis can then be used to perform wavefront shaping by changing its basis to a SLM pixel basis. This enables to perform imaging or telecommunications with MMFs but isn't enough for high energy applications where non linear effects perturb the modal composition and deteriorate the signal. Being able to control the signal modes and their propagation could allow to solve this kind of problems and amplified MMFs might be the way to achieve this kind of control.

Simulating the propagation of light through a MMF

The influence of amplification is described by a theoretical model that is based on the modal behavior of the pump and signal beams in the fiber and population inversion induced by the amplification that applies to each mode of the signal. To investigate the influence of amplification on the signal's modal composition, finite elements simulations were used. The field corresponding to the pump beam which propagates in the direction opposed to the one of the signal beam is calculated in the whole fiber and the transmission matrix is deduced by multiplying the ones of several subdivisions, calculated with the model further exposed. Since it had to be possible to simulate the influence of many different pumps to perform optimization, a trade-off between memory and computation time and an efficient implementation were studied.

2.1 The model

The methods exposed in 1.2 can be extended to Multimode Fiber Amplifiers, where the amplifying beam excites new modes and transforms the Transmission Matrix. The model explained further describes the relation between the pump intensity and the stimulation of signal modes during the propagation of a pump beam.

2.1.1 Incoming beam in a MMF

When a light field enters a MMF, it can be considered as decomposed on the modal basis of the fiber. All those modes then propagate the way predicted by the equations of Section 1. We also explained the meaning of the following expression in 1.2.2:

$$E(x, y, z) = \sum_i \alpha_i \psi_i(x, y, z) + \left(E(x, y, z) - \sum_i \alpha_i \psi_i(x, y, z) \right) \quad (2.1)$$

and if we assume the incoming field is a sum of LP guided modes only, it becomes

$$E(x, y, z) = \sum_i \alpha_i \psi_i(x, y, z) \quad (2.2)$$

The number of modes in a given fiber can be computed by solving equation (1.26) or by using the approximations of Section 1.1.4. To effectively and efficiently compute those parameters, the method being used in the simulations is the one outlined by Mitschke in [5]. His method is based on the fact that when computing the solutions, the

values of u satisfying (1.26) can be grouped in pairs. This can be intuitively understood with Figure 1.4. In practice, the solutions for LP_{01} and LP_{11} will be searched for first, then LP_{02} and LP_{12} if they exists, moving to $\ell = 3$ and $\ell = 4$ if they don't, etc. The code implementing this method for the simulation is in Listing A.1.

Space can be discretised for the simulation in both the transverse plane and longitudinal dimension. E can be written in all the fiber with equation (1.25), assuming that there is no absorption of light in the fiber material. For fibers with lengths of the order of 1 m, this approximation is satisfying enough. The obtained values for the light field are valid for both a propagating signal beam and a pump beam, ensuring the z -axis is inverted with the latter.

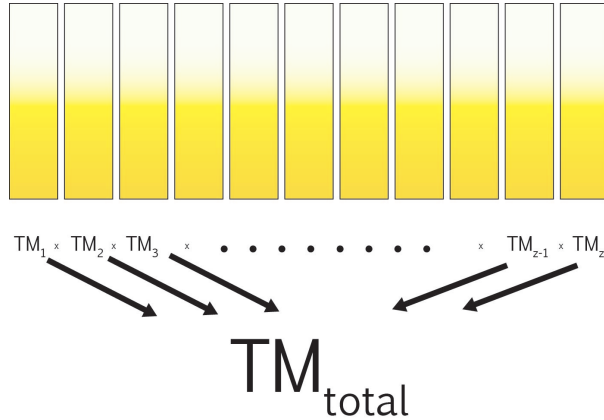


Figure 2.1 – Diagram of the Transmission Matrix calculation division and recombination

The length of the discretisation must ensure that no information is lost about the pump beam, which will be used to calculate the transmission matrix. For this, the discretisation length must be smaller than the smallest dephasing length between two modes of the propagating pump. That is

$$\Delta z < DL_{pump} \quad (2.3)$$

where DL is defined as in (1.41).

2.1.2 Rare-earth amplified fiber

The work I carried out focuses on Multimode Fiber Amplifiers (MMFA) and more precisely Ytterbium-doped fibers. As shown on Figure 2.3, Ytterbium MMFA are experimentally amplified by adding a pump beam of different wavelength which will excites the Yb atoms and trigger lasing and amplification of the propagating signal.

Light enters the fiber with a certain amount of energy and is then amplified by stimulated emission. The pump propagating, similarly to the signal, with modal components, the population inversion of Yb atoms is non uniform and therefore has a more complex effect than uniformly amplifying the signal. With a given modal decomposition of the signal at some z in the fiber, the amplification will occur on each mode but non uniformly spatially on the corresponding cross-section of the fiber. It is assumed that the obtained amplified field can then be decomposed again on the basis of the signal modes of the fiber and that the process can be repeated at $z + dz$.

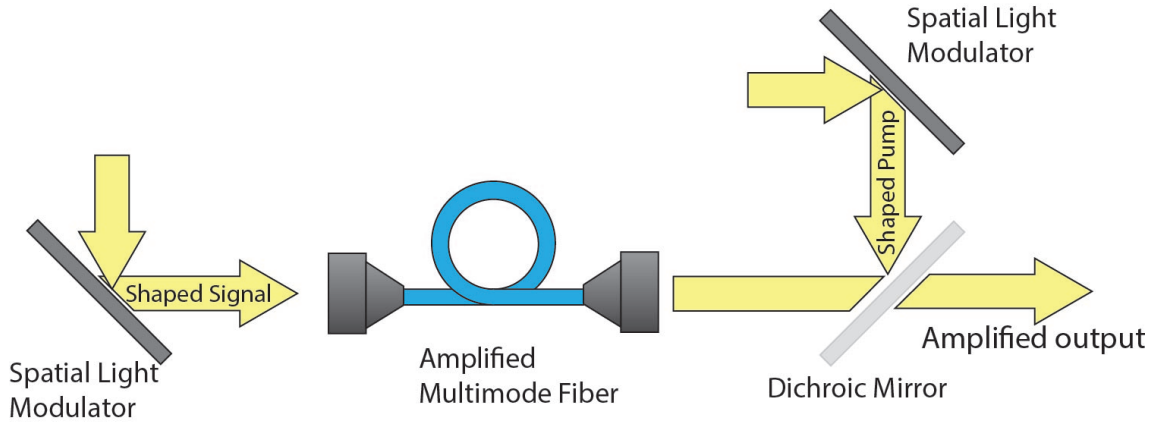


Figure 2.2 – Diagram of a MMFA setup for visualizing the influence of a shaped pump beam on the fiber transmission matrix. The pump beam enters the fiber on the side opposite to the signal input. A dichroic mirror enables to retrieve the fiber output.

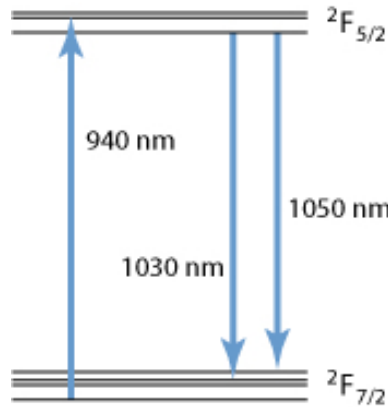


Figure 2.3 – Diagram of energy levels of Yb^{3+} ions and the usual pump and laser transitions. Here the pump beam of wavelength 940 nm triggers population inversion and stimulated emission with the signal beam of wavelength 1040 nm [6].

This central part of the model can be written in equations : if

$$E_{in}|_z = \psi_{s,i}(x, y) \quad (2.4)$$

is the input field having components one only one signal mode $\psi_{s,i}$ at coordinates x, y, z , the output field at $x, y, z + dz$ is written

$$E_{out}|_{z+dz} = \underbrace{e^{i\beta\Delta z}\psi_{s,i}(x, y)}_{\text{passive propagation of the mode}} + \underbrace{\sum_j^N \alpha_j(z)\psi_{s,j}(x, y)}_{\text{amplified part of the signal decomposed on all the signal modes}} \quad (2.5)$$

where $\alpha_j(z)$ is

$$\alpha_j(z) = g_{Yt} i\beta_i \Delta z e^{i\beta_i \Delta z} \iint I_{pump}(x', y', z) \psi_{s,i}(x', y') \psi_{s,j}^*(x', y') dx' dy' \quad (2.6)$$

The term g_{Yt} is a complex-gain coefficient. It links the pump intensity and the amplification and phase-shift of the signal field depending on the signal and pump wavelengths. The absorption and gain spectrum of the Ytterbium is described in [7] and the corresponding phase-shift is obtained with the Kramers-Kroning relations [1].

It is not surprising to see that if $I_{pump} = 0$ is equals to 0 in (2.6), equation (2.5) becomes $E_{out}|_{z+dz} = e^{i\beta\Delta z}\psi_{s,i}(x, y)$, the regular expression for propagation of a mode in a fiber slice of length Δz . Furthermore, if I_{pump} is uniform on every cross-section, all the integrals in (2.6) are equal to 0 for $i \neq j$ because the modes are orthogonal. The modes would be in that case only self-amplified according to the intensity of the pump (the transmission matrix would then be diagonal). Therefore, the influence of the pump beam is interesting when it is non-uniform, that is to say when the integrals of (2.6) aren't 0 and when some amplified modes excite others in the signal.

2.2 The simulation and its challenges

This section describes how the simulation was implemented and what were the technical and computational difficulties encountered. Different issues have strongly influenced the simulation and the realisation of optimization on powerful computers to make it possible to simulate many realisations of different modal compositions of the pump to compare the resulting transmission matrices and find interesting links between certain pump configuration and specific effects on the signal.

To have a rough idea of the computational resources needed for running the simulation, we can estimate the size of the data needed to simulate the whole fiber at once and calculate the resulting transmission matrix. First, the typical order of magnitude of the fiber amplifier's parameters are $\lambda_{signal} = 1030nm$, $\lambda_{pump} = 975nm$, $NA = 0.16$, $a = 15\mu m$ (core radius), $n_1 = 1.5$, $L = 5cm$. This corresponds to 59 propagable modes for the pump and 52 propagable modes for the signal. The size of the (x, y) spatial discretisation had to be chosen to be the smallest possible without losing too much information on the pump wave's intensity profile. The threshold arbitrarily chosen was between 5 and 10 pixels (space elements) per spot on the speckle pattern, which corresponds for the 59 modes of the pump to approximately 200 spatial points in each direction of a cross-section of a fiber. The z -axis discretization was chosen to be 1/6th of the global dephasing length (the smallest dephasing length between all the modes of the pump), value beyond which the distance (in the sense of the max norm) between a matrix simulated with this step and an other with a smaller one is smaller than 10^{-5} . For a dephasing length of typically $10\mu m$ and a $5cm$ long fiber (rather small compared to MMFA commonly used for regular applications) there are 5000 slice to use and thus 5000 transmission matrices to calculate and recombine to get the final transmission matrix.

The number of integrals (2.6) to be calculated is equal to $N(N - 1)/2$ where N is the number of signal modes, in this case 1326 couplings between modes. Since the array containing all the fields on the grid at $z = 0$ are used in all the integrals, it is kept for all the simulation to avoid recalculating it. All the fields are complex scalar and every element is stored on 128 bits in python. The biggest and most expansive array from a memory point of view is the one in which the integral is calculated. Since the resulting local matrices for a slice can be calculated independently from one another, it is theoretically possible to directly compute all the integrals corresponding not only to all the couplings in a slice of fiber but also to the all the slices of the fiber

simultaneously. The size of the array would then add up to

$$\underbrace{1326}_{\text{number of couplings}} \cdot \underbrace{5000}_{\text{number of slices}} \cdot \underbrace{(200 \cdot 200)}_{\text{number of spatial points}} \cdot \underbrace{128}_{\text{number of bits per elements}} = 35.2\text{TB} \quad (2.7)$$

This number is excessively big even for computer clusters and we therefore quickly abandoned the idea of performing single shot calculations of transmission matrices. If we do the same calculation one fiber slice at a time the size of the array to be handled is down to 7GB. This number is still quite big for regular computers but is acceptable for simulation computers with RAM between 32GB and 96GB. Yet, the native implementation of sum and product functions in python not being well optimized for multicore CPUs, each slice was taking approximately 1 second to be calculated that is 1 hour and a half for each matrix. Optimization would need to be able to test at least every mode in the pump and would be efficient with much more realisations. To be able to perform optimization, the code was parallelized over the multiple core of a CPU. Slices are equally partitioned and each batch is processed by a single core sequentially. The corresponding code for parallelizing is in Appendix A Listing A.2. It made it possible to calculate a whole 5cm fiber's transmission matrix in only 1 minute 30 seconds and to evaluate much more realization of pump configurations.

The optimization that was selected does a scan of all the modes one by one. The starting point is a random pump configuration, with a weight of 1 for all the modes and a random phase for each one of them. This decision was based on the assumption that the influence of the phase on the overall transmission matrix was negligible. It had been investigated with test simulations early on in the work. The program then looks at each mode and tries to change it's weight to 0.3, 0.6, 0.9 and 1.2 and keeps the best configuration before going on to the next mode. The algorithm converged after between 2 and 3 scans of all the modes, that is between 472 and 708 transmission matrices' calculations.

Results of the simulations

Since a single optimization scan takes at least 6 hours to run, we had to select some particular elements we were going to look at and which we tried to maximize. Not all the elements showed a possibility to be maximized with the optimization algorithm, but some of them reacted significantly, exhibiting other behaviors on related modes. Significant minimization of diagonal elements was observed, suggesting the possibility to tune amplification specifically to disable entirely one mode channel. The phenomenon of extinction was also linked in some cases with an intermodal coupling which has also been investigated with simulations.

3.1 Maximizing an off diagonal element

The results of Figure 3.1 were obtained when running the optimization algorithm with the objective of minimizing the cost function

$$J(\text{pump}) = - \left| \frac{\text{TM}_{\text{pump}}[10, 13]}{\text{TM}_{\text{pump}}[13, 13]} \right| \quad (3.1)$$

where pump can be represented by a vector of size 59 containing complex numbers $(w_k e^{i\theta_k})_{k \in \{1 \dots 59\}}$ with w_k the weight assigned to mode k and θ_k its randomly initialized phase.

$J(\text{pump})$ is a function of all the weights assigned to the pump modes for a given set of fiber parameters. The relation is strongly non linear in the pump weights because of the intensity term I_{pump} in (2.6). It is therefore very hard to predict or even approximate the influence of each "dimension" of the pump space and to be able to perform regular optimization methods on the pump. Even a systematic exploration of this discretized space would be far too time consuming, because one scan of all the possible configurations would mean computing $(\text{number of possible weights})^{\text{number of modes}}$ transmission matrices. That is, for the typical configurations studied here, 3^{59} or 4^{59} transmission matrices.

At each iteration, the algorithm perturbs the weight of a mode and keeps the perturbation that results in the lowest cost function value (which can be no perturbation at all). $J(\text{pump})$ is the ratio of $\text{TM}_{\text{pump}}[10, 13]$ and $\text{TM}_{\text{pump}}[13, 13]$ rather than only $\text{TM}_{\text{pump}}[10, 13]$ to take into account the "channel 13 to channel 13" transmission and to compare how much amplification of mode 13 triggers mode 10 instead of mode 13 itself.

Figure 3.1 shows two optimization examples. The simulation was stopped after two scans on both examples ; it was very progressive and slow at the beginning and then only improves by large amounts and sporadically from the beginning of the second scan

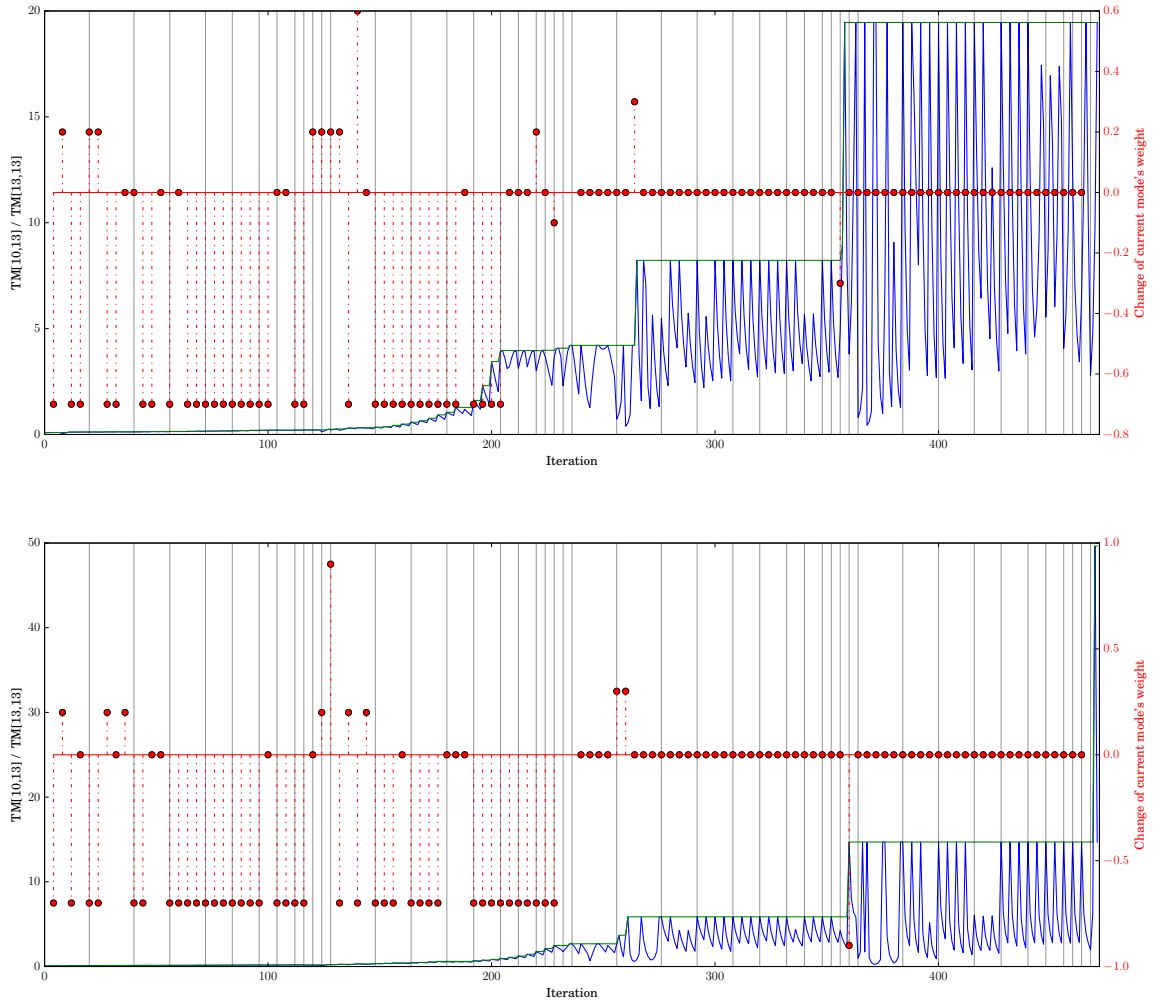


Figure 3.1 – Two optimization results for maximizing target element $\text{TM}[10, 13]$. The blue curve represents the value of the cost function at a given iteration. The green curve is the best result so far and the red handles represent the corresponding change of a mode’s weight for a newly selected best pump configuration.

until the end of optimization. By looking at the red circles we notice that most of the modes were turned down during the optimization process. Some others were kept and likely account for the results obtained.

In both cases, after the end of first scan the value of $J(\text{pump})$ (for purpose of clarity, $-J(\text{pump})$ is plotted in Figure 3.1) gets very unstable, meaning that a minima has been reached. The first minima corresponds to $J(\text{pump}) = 19.5$, that is element [10,13] is in absolute value 19.5 times larger than element [13,13] that traduces the mode 13’s component of an output when mode 13 is the only input. The results were impressive given the fact that in preliminary simulations we only observed slight perturbation of the transmission matrix but never such significant ratio between an off-diagonal element and a diagonal element.

The first and final pump configurations for each optimization case are shown in Figure 3.2. A trend appears clearly with the majority of modes being turned down to a weight of 0.3 (the minimum possible value for the algorithm). Some modes have

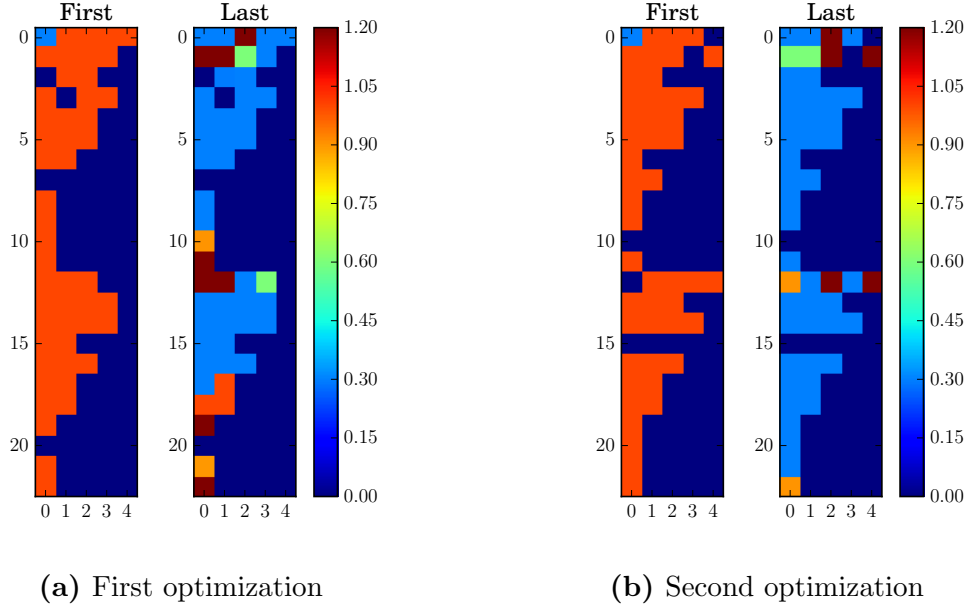


Figure 3.2 – First and final pump configuration for the two optimization cases of Figure 3.1. The modes are indexed from 0 in both directions (LP_{01} becomes LP_{00}). Some randomly selected modes are turned off for each simulation.

therefore more influence on particular elements of the matrix than other and they seem to be similar from one simulation to another which could lead to insightful relations between pump modes and signal modes.

Not all the simulations showed such impressive results for maximization of off-diagonal elements of the transmission matrix. Some of them didn't show off-diagonal to diagonal ratios superior than 1 but were nonetheless significantly decreased. Figure A.1 in Appendix shows two examples of significant optimizations of element [15, 30] with the ratio $\left| \frac{\text{TM}_{\text{pump}}[10,13]}{\text{TM}_{\text{pump}}[13,13]} \right|$ going from 0.01 to 0.17 in the first case and to 0.39 in the second case. Figure A.2 of Appendix shows quite different first and final pump configurations, perhaps meaning that the cost function minima isn't as well defined as for element [10,13].

3.2 Minimizing a diagonal element

When looking closer at the results of optimization processes aiming for the minimization of

$$J(\text{pump}) = - \left| \frac{\text{TM}_{\text{pump}}[a, b]}{\text{TM}_{\text{pump}}[b, b]} \right| \quad (3.2)$$

we noticed that the minimization was sometimes not only driven by the maximization of $|\text{TM}_{\text{pump}}[a, b]|$ but also (and sometimes almost only) by the minimization of $|\text{TM}_{\text{pump}}[b, b]|$. This phenomenon was very surprising since the overall effect of the pump propagation on a relatively long fiber was expected to "average out" and the self-amplification of each mode was supposed to stay strong.

We then tried to optimize with the following cost function to study more precisely

the minimization of diagonal elements in the fiber :

$$J(\text{pump}) = |\text{TM}_{\text{pump}}[b, b]| \quad (3.3)$$

First, we optimized on element [13,13] to confirm what had been observed when trying to maximize [10,13]. As for the first case, two optimizations with two different random starting points were performed to verify the relative importance of the initial phase of the pump modes.

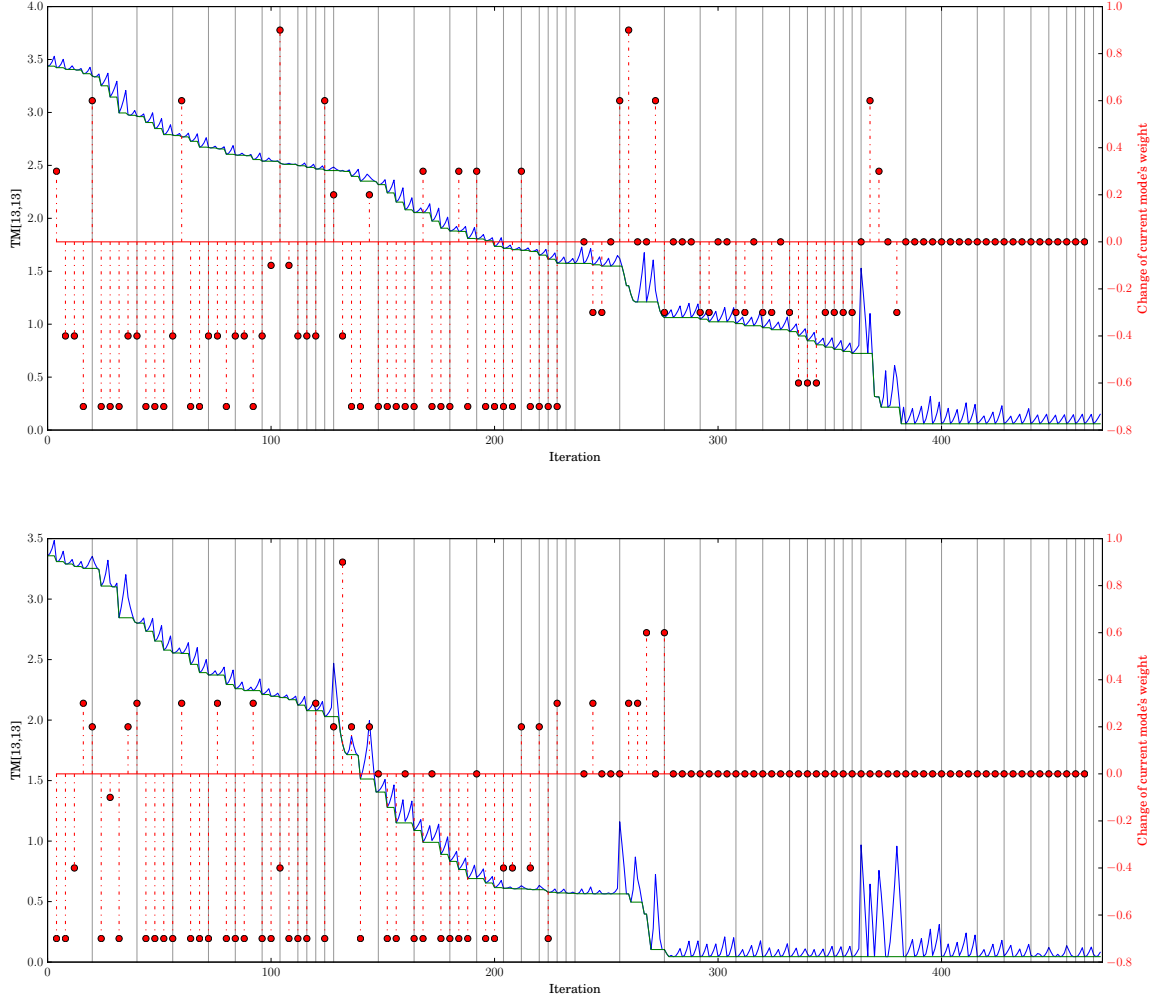


Figure 3.3 – Two optimization results for minimizing target element $\text{TM}[13, 13]$. The blue curve represents the value of the cost function at a given iteration. The green curve is the best result so far and the red handles represent the corresponding change of a mode's weight for a newly selected best pump configuration.

The results are shown on Figure 3.3 where it becomes clear that it is possible to minimize element [13,13] and reduce it from 350% of input mode 13 being found in mode 13 at the output to less than 10%. It means that when mode 13 is sent in the fiber with such a pump, less than 10% of input intensity is retrieved on mode 13 at the output. Those 35 fold improvements account for the results obtained with the ratio $\left| \frac{\text{TM}_{\text{pump}}[10,13]}{\text{TM}_{\text{pump}}[13,13]} \right|$.

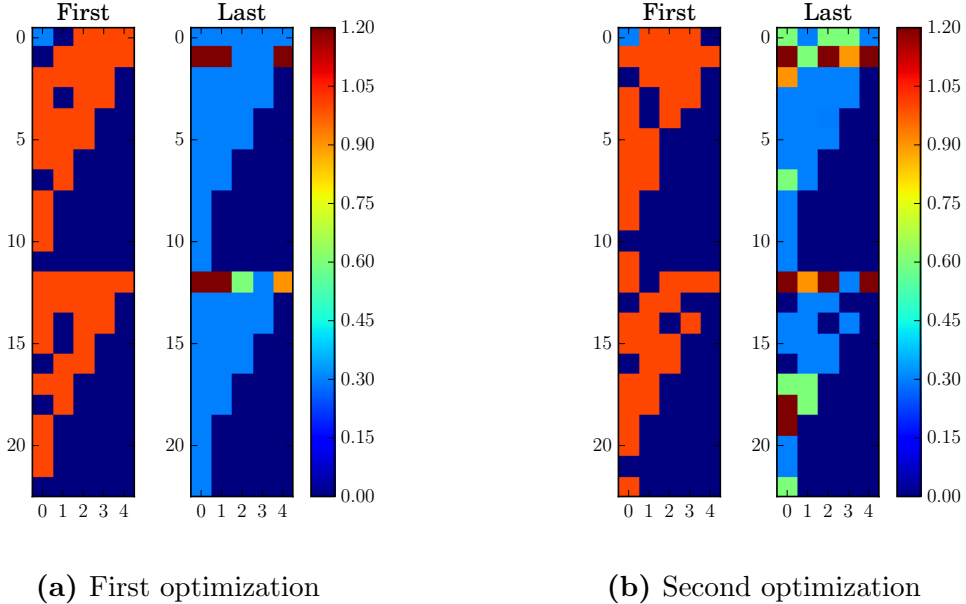


Figure 3.4 – First and final pump configuration for the two optimization cases of Figure 3.3. The modes are indexed from 0 in both directions (LP_{01} becomes LP_{00}). Some randomly selected modes are turned off for each simulation.

Figure 3.4 shows the pump configurations for the two optimization cases. There are some similarities with the pump configurations obtained when optimizing on element [10,13] and there is no doubt that when trying to minimize the above ratio, the optimization naturally tended to minimize element [13,13].

This phenomenon is far from general and isn't true for most of the elements of the transmission matrix. With other simulations on elements [10,10], [12, 12] or [43, 43] for example (the corresponding results are in Appendix), no below 100% values were observed for the diagonal element. This might even be only an isolated phenomenon affecting only one or two modes.

3.3 Intermodal coupling

The phenomenon of minimization of some diagonal elements implies that the input and amplification energy of those modes is displaced to others. After observing the transmission matrices, it appeared that this energy wasn't equally distributed over the other modes. It was rather concentrated on one particular mode as shown on Figure 3.5.

When mode element [13,13] is minimized, element [39, 39] is also minimized and elements [13, 39] and [39, 13] are correspondingly maximized. There is therefore a strong coupling between mode 13 and 39 which are closely related because they are the odd and even counterpart of each other where odd and even correspond to the two polarization states mentioned in section 1.14. This link can also be visualized with the graph of Figure 3.6 where the absolute gain of $LP_{1,2,even}$ and $LP_{1,2,odd}$ is plotted as a function of the length of the fiber. The pump configurations obtained with optimization for 50mm corresponds to a minimum of gain for $LP_{1,2,even}$ and the gain is transferred to its counterpart during transmission in the fiber.

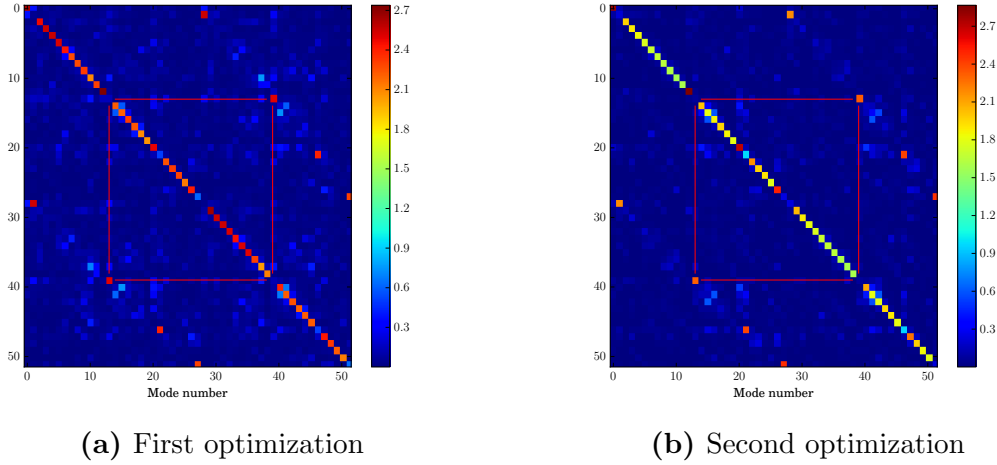


Figure 3.5 – Final transmission matrices for the two optimization cases of 3.1. Red lines emphasize the link between odd and even counterparts of the mode being minimized

This coupling was also observed for other pairs of modes but it seems to be linked with minimization of self amplification of the corresponding modes. However, many modes (especially LP_{0m} modes that don't have the degeneracy mentioned above) didn't exhibit the same characteristics.

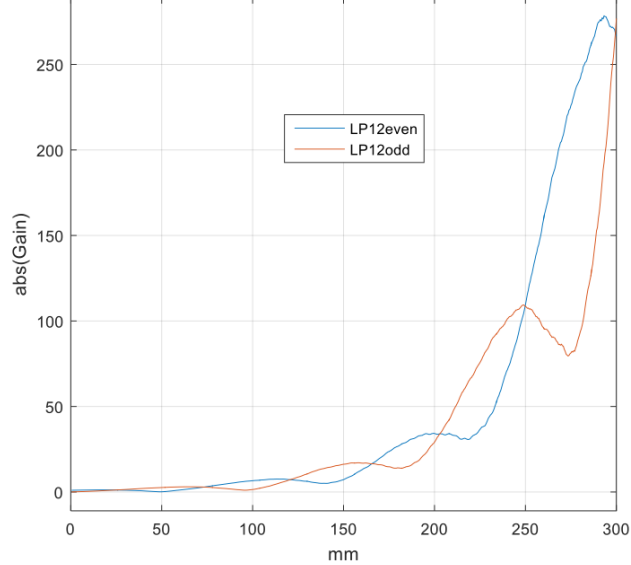


Figure 3.6 – Absolute gain on mode 13 and 39 as a function of the length of the fiber. There is an oscillating coupling between the two modes which drives the minimization of element [13,13] in the example above.

Conclusion

The influence of amplification on the behavior of light in multimode fibers is still very complicated and unpredictable. The whole theory it is based on is well understood and has very good results for regular fibers but the extension of the theory to amplified fibers yields new surprising and complex phenomena mainly because of the non linearity induced by the amplifier. A way to investigate the effects of amplification is to simulate light propagation and compute the transmission matrix of an amplified multimode fiber with the model described in the report. This simulation posed major problems of scale to be able to use it to perform optimization and necessitated particular implementation and hardware. The results gave new insights in the theory, showing that particular pump configurations could achieve very specific behavior of the transmission matrix, namely maximization of some elements and minimization of diagonal elements. The latter was linked to a coupling between similar modes, leading to new questions about the possibility to control light propagation in multimode fiber by shaping the pump beam.

The control of amplification in fiber amplifiers with Spatial Light Modulators could allow to verify experimentally those results and to get a better understanding of this behavior. Moreover, there is still investigation to be done on the optimization process to try more complex target than a single element of the transmission matrix and to see if refining the grid search on the pump modes could lead to better results.

Bibliography

- [1] John W. Arkwright et al. “Experimental and Theoretical Analysis of the Resonant Nonlinearity in Ytterbium-Doped Fiber”. In: *J. Lightwave Technol.* 16.5 (1998), p. 798. URL: <http://jlt.osa.org/abstract.cfm?URI=jlt-16-5-798>.
- [2] John A. Buck. *Fundamentals of Optical Fibers*. Ed. by Bahaa E. A. Saleh. Second. John Wiley And Sons, Inc., 2004.
- [3] Sylvain Gigan. “Optical microscopy aims deep”. In: *Nat Photon* 11.1 (Jan. 2017), pp. 14–16. URL: <http://dx.doi.org/10.1038/nphoton.2016.257>.
- [4] D. Gloge. “Weakly Guiding Fibers”. In: *Appl. Opt.* 10.10 (1971), pp. 2252–2258. DOI: 10.1364/AO.10.002252. URL: <http://ao.osa.org/abstract.cfm?URI=ao-10-10-2252>.
- [5] Fedor Mitschke. *Fiber Optics. Physics and Technology*. 1st ed. Springer-Verlag Berlin Heidelberg, 2010. DOI: 10.1007/978-3-642-03703-0.
- [6] R. Paschotta. “article on ‘Ytterbium-doped Gain Media’”. In: *Encyclopedia of Laser Physics and Technology* (2006).
- [7] R. Paschotta et al. “Ytterbium-doped fiber amplifiers”. In: *IEEE Journal of Quantum Electronics* 33.7 (1997), pp. 1049–1056. ISSN: 0018-9197. DOI: 10.1109/3.594865.
- [8] Martin Plöschner, Tomáš Tyc, and Tomáš Čižmár. “Seeing through chaos in multimode fibres”. In: *Nat Photon* 9.8 (Aug. 2015), pp. 529–535. URL: <http://dx.doi.org/10.1038/nphoton.2015.112>.
- [9] S. M. Popoff et al. “Measuring the Transmission Matrix in Optics: An Approach to the Study and Control of Light Propagation in Disordered Media”. In: *Phys. Rev. Lett.* 104 (10 2010), p. 100601. DOI: 10.1103/PhysRevLett.104.100601. URL: <http://link.aps.org/doi/10.1103/PhysRevLett.104.100601>.
- [10] Sébastien Popoff et al. “Image transmission through an opaque material”. In: *Nature Communications* 1 (Sept. 2010), 81 EP –. URL: <http://dx.doi.org/10.1038/ncomms1078>.
- [11] Brandon Redding et al. “High-resolution and broadband all-fiber spectrometers”. In: *Optica* 1.3 (2014), pp. 175–180. DOI: 10.1364/OPTICA.1.000175. URL: <http://www.osapublishing.org/optica/abstract.cfm?URI=optica-1-3-175>.
- [12] A. N. Tikhonov. *Solution of incorrectly formulated problems and the regularization method*. Soviet Math. Dokl., 1963, pp. 1035–1038.
- [13] I. M. Vellekoop and A. P. Mosk. “Focusing coherent light through opaque strongly scattering media”. In: *Opt. Lett.* 32.16 (2007), pp. 2309–2311. DOI: 10.1364/OL.32.002309. URL: <http://ol.osa.org/abstract.cfm?URI=ol-32-16-2309>.

- [14] E. Weisstein. “Bessel Differential Equation.” In: *From MathWorld—A Wolfram Web Resource* (2010).
<http://mathworld.wolfram.com/BesselDifferentialEquation.html>.
- [15] E. Weisstein. “Modified Bessel Differential Equation.” In: *From MathWorld—A Wolfram Web Resource* (2010).
<http://mathworld.wolfram.com/ModifiedBesselDifferentialEquation.html>.

Appendix

Listing A.1 – Find u solutions by Mitschke

```

# -*- coding: utf-8 -*-
"""
Created on Mon Sep 26 18:08:23 2016
@author: Hugo
"""

import scipy.special as spec
import numpy as np
import scipy as sc
from CharFunForLP import CharacteristicFunctionForLP

def Find_u_Solutions_by_Mitschke(V, eps=1e-12):
    """
    Inputs a V number of an optical fiber and a desired precision eps and
    outputs a list of the u solutions of the eigenvalue equation along with the
    L and M values associated with the LP modes.
    """
    u_values = np.zeros((100, 100))
    L_values = np.zeros((100, 100))-1
    M_values = np.zeros((100, 100))-1
    l = 0
    NumOfZerosCeil = round(V/2)
    GoOn = True

    while GoOn:
        EvenZeros = spec.jn_zeros(l, NumOfZerosCeil)
        OddZeros = spec.jn_zeros(l+1, NumOfZerosCeil)

        StopInd = np.nonzero(EvenZeros > V)[0][0]
        if StopInd == 0:
            GoOn = 0
        else:
            for m in range(0, StopInd):
                if m == 0:
                    LeftLimit = 0
                else:
                    LeftLimit = OddZeros[m-1]
                u_0 = (LeftLimit + min(V, EvenZeros[m]))/2

                def tempF(u, V, l):
                    return CharacteristicFunctionForLP(u, V, l)

                u_solution = sc.optimize.fsolve(lambda u: tempF(u, V, l), u_0)

                if CharacteristicFunctionForLP(u_solution, V, l) <= eps:
                    u_values[l, m] = u_solution
                    L_values[l, m] = l
                    M_values[l, m] = m+1

                u_0 = (EvenZeros[m]+min(V, OddZeros[m]))/2

                u_solution = sc.optimize.fsolve(lambda u: tempF(u, V, l+1),
                                                u_0)
                if CharacteristicFunctionForLP(u_solution, V, l+1) <= eps:
                    u_values[l+1, m] = u_solution
                    L_values[l+1, m] = l+1
                    M_values[l+1, m] = m+1

            print('u_values_for_LP'+str(l)+', '+str(m+1) +
                  '; LP'+str(l+1)+', '+str(m+1)+'-done')

        l = l+2
        nonZeroUL = np.nonzero(u_values[:, 0])[0]
        nonZeroUM = np.nonzero(u_values[0, :])[0]

        l_max = nonZeroUL[len(nonZeroUL)-1]
        m_max = nonZeroUM[len(nonZeroUM)-1]

        u_values = u_values[0:l_max+1, 0:m_max+1]
        L_values = L_values[0:l_max+1, 0:m_max+1]

```

```

M_values = M_values[0:l_max+1, 0:m_max+1]
return (u_values, L_values, M_values)

```

Listing A.2 – Calculate Transmission Matrix Parallelly

```

#-*- coding: utf-8 -*-
"""
Created on Sat Oct 1 11:29:11 2016
@author: Hugo
"""

import numpy as np
from ArrangeModeMatrixAsList import ArrangeModeMatrixAsList
import sys
import numexpr as ne
import multiprocessing as mp
"""
This functions gives the matrix for which every element is the minimum value
between the same element in a and p
"""

def matdot(A, B):
    C = np.zeros(np.shape(A))+0j
    for i in range(np.shape(A)[0]):
        for j in range(np.shape(A)[1]):
            C[i, j] = np.sum(A[i, :]*B[:, j])
    return C

def findMinimum(a, p):
    a = a[:, :, np.newaxis]
    p = np.zeros(np.shape(a))+p
    return np.amin(np.concatenate((a, p), axis=2), axis=2)

"""
This function superposes the fields of a stack after making them propagate of
z_in_um with the propagations constants of ComplexAmp_p
"""

def SuperposeModeFields(ModeFieldStack, BetaStack, z_in_um, ComplexAmp_p):
    SummedField = np.sum(ModeFieldStack*np.exp(-1e-6*j*BetaStack*z_in_um) *
                         ComplexAmp_p, axis=2)
    return SummedField

"""
This function applies the Ytterbium Gain Model to the Pump Intensity field in
in order to output a complex refractive index which affect every overlapped
mode of the signal
"""

def YtterbiumComplexGainModel(PumpIntensity):
    YbConcentration = 1e26
    lbd = 1030e-9
    RIC_imag = 6.2734e-25*(lbd/2*np.pi)*YbConcentration
    RIC_real = 2.2513e-32*YbConcentration
    RIC_real = (7.4/0.22)*RIC_real
    ComplexRefractiveIndex = (RIC_real+j*RIC_imag)
    PumpIntensity = findMinimum(PumpIntensity, 1)
    ComplexRefractiveIndex *= (PumpIntensity-0/10)
    return ComplexRefractiveIndex

"""
This function takes the vector of all the possible coupling of signal modes
amplification profiles and puts it into the form of a transmission matrix
"""

def ArrangeListToHermitianMatrix(vec, N):
    if np.size(vec) != N*(N+1)/2:
        print("Error_in_ArrangeListTOHermitian")
        T = []
        return T
    else:
        Mat = np.zeros((N, N))
        Mat = Mat+0j
        for r in range(N):
            eb = (r+1)*N-(r)*(r+1)/2
            eb = int(eb)
            sb = eb - (N-(r+1))
            Mat[r, r:N] = vec[sb-1:eb]
        Mat_no_diag = Mat-np.diag(np.diag(Mat))

```

```

Mat = Mat_wo_diag + np.conj(np.transpose(Mat_wo_diag)) + np.diag(np.diag(Mat))
return Mat

"""
Some functions to multiply the two big arrays in different ways (testing).
The method currently used is numexpr
"""

def MatrixMultip(A, B):
    return A*B

def MultipAndSum(A, B):
    return np.sum(np.multiply(A, B), axis=(0, 1))

def numexprmultAndSum(X, Y):
    return np.sum(ne.evaluate("X*Y"), axis=(0, 1))

"""
sliceUp divides the time and memory consuming calculations into smaller chunks
which are summed separately into the resulting array
"""

def sliceUp(X, Y, n):
    step = round(np.size(X[0, 0, :]) / n)
    result = np.zeros_like(X[0, 0, :]) + 0
    for i in range(0, np.size(X[0, 0, :]), step):
        result[i:i+step-1] += numexprmultAndSum(X[:, :, i:i+step-1], Y)
    return result

def sliceCalc(ModeFieldStack_p, BetaStack_p, ComplexAmp_p, L, MultipFactorIp,
             SubZaxis, PassiveTM, UniformGainTM, ModeCoupling_s,
             NumberOfSignalModes, currentID, count):
    print("Slice_" + str(count) + " entered")
    sys.stdout.flush()
    LocTransmissionMatrix = np.eye(np.shape(PassiveTM)[0])
    SaturationCounter = 0
    for z in range(np.size(SubZaxis)):
        PumpField = SuperposeModeFields(ModeFieldStack_p, BetaStack_p,
                                         -L+SubZaxis[z], ComplexAmp_p)
        Ip = PumpField * np.conj(PumpField)

        PopulationInversion = MultipFactorIp * Ip
        SaturationCounter += np.size(np.nonzero(PopulationInversion > 1)[0])
        ComplexRefractiveIndex = YtterbiumComplexGainModel(PopulationInversion)
        ComplexRefractiveIndex = ComplexRefractiveIndex[:, :, np.newaxis]

        GMatrix = ArrangeListToHermitianMatrix(numexprmultAndSum(
            ModeCoupling_s, ComplexRefractiveIndex), NumberOfSignalModes)
        tm = PassiveTM + GMatrix * UniformGainTM
        LocTransmissionMatrix = matdot(tm, LocTransmissionMatrix)

        if (z % 70 == 0):
            print(str(count) + ' ' + str(100 * z / np.size(SubZaxis)) + ' done')
            sys.stdout.flush()
    print("Slice_" + str(count) + " finished")
    sys.stdout.flush()
    np.save('subMat' + str(currentID) + '/mat' + str(count) + '.npy',
           LocTransmissionMatrix)

"""
The main function which calculates the transmission matrix with a given set of
parameters
"""

def CalculateTransmissionMatrix(ComplexAmp_p, MultipFactorIp, dz, i, k,
                                 pump, numbModes, proc_name, currentID):
    print("Entered " + str(i) + str(k) + str(pump) +
          str(numbModes) + ' ' + str(proc_name))
    sys.stdout.flush()
    file = np.load("currentFile.npz")
    L = file['L']
    Xaxis = file['Xaxis']
    Yaxis = file['Yaxis']
    beta_mat_p = file['beta_mat_p']
    beta_mat_s = file['beta_mat_s']
    ModeFieldStack_p = file['ModeFieldStack_p']
    ModeCoupling_s = file['ModeCoupling_s']
    file.close()
    print(proc_name + ' loaded')
    sys.stdout.flush()

    Nstep = int(np.ceil(L/dz))
    dz1 = L/Nstep
    Xaxis = np.arange(0, L+dz1, dz1)

    Sy = np.size(Yaxis)
    Sx = np.size(Xaxis)

    BetaStack_p = ArrangeModeMatrixAsList(beta_mat_p, beta_mat_p)
    BetaStack_p = np.reshape(BetaStack_p, (1, 1, np.size(BetaStack_p)))

```

```

ComplexAmp_p = ArrangeModeMatrixAsList(ComplexAmp_p, beta_mat_p)
ComplexAmp_p = ComplexAmp_p[np.newaxis, np.newaxis, :]

DoubleBeta_s = ArrangeModeMatrixAsList(beta_mat_s, beta_mat_s)

NumberOfSignalModes = np.size(DoubleBeta_s)

expVar = np.exp(-1j*dz1*1e-6*DoubleBeta_s)
PassiveTM = np.diag(expVar)

UniformGainTM = -1j*dz1*1e-6*DoubleBeta_s*expVar
UniformGainTM = np.reshape(UniformGainTM, (1, np.size(UniformGainTM)))

TransmissionMatrix = np.eye(np.shape(PassiveTM)[0])

SaturationCounter = 0
Zaxiscut = Zaxis[1:]
sliceLength = np.size(Zaxiscut)//mp.cpu_count()+1
count = 0
procList = []
for n in range(mp.cpu_count()):
    SubZaxis = Zaxiscut[n*sliceLength:(n+1)*sliceLength]
    proc = mp.Process(target=sliceCalc,
                       args=(ModeFieldStack_p, BetaStack_p, ComplexAmp_p, L,
                              MultipFactorIp, SubZaxis, PassiveTM,
                              UniformGainTM, ModeCoupling_s,
                              NumberOfSignalModes, currentID, count))
    procList.append(proc)
    proc.start()
    print('proc-' + str(count) + ' started')
    sys.stdout.flush()
    count += 1
for proc in procList:
    proc.join()

for n in range(count):
    tm = np.load('subMat' + str(currentID) + '/mat' + str(n) + '.npy')
    TransmissionMatrix = matdot(tm, TransmissionMatrix)

print(proc_name + ': ' + 'Saturation_was_ ' +
      str(100*SaturationCounter/(Nstep*0.78*Sx*Sx)) + '%')
np.savez("Data"+str(currentID)+"/currentMat"+str(i)+"_"+str(k)+"," +
         str(pump)+"_"+str(numModes)+".npz",
         TransmissionMatrix=TransmissionMatrix,
         ComplexAmp_p=ComplexAmp_p)

```

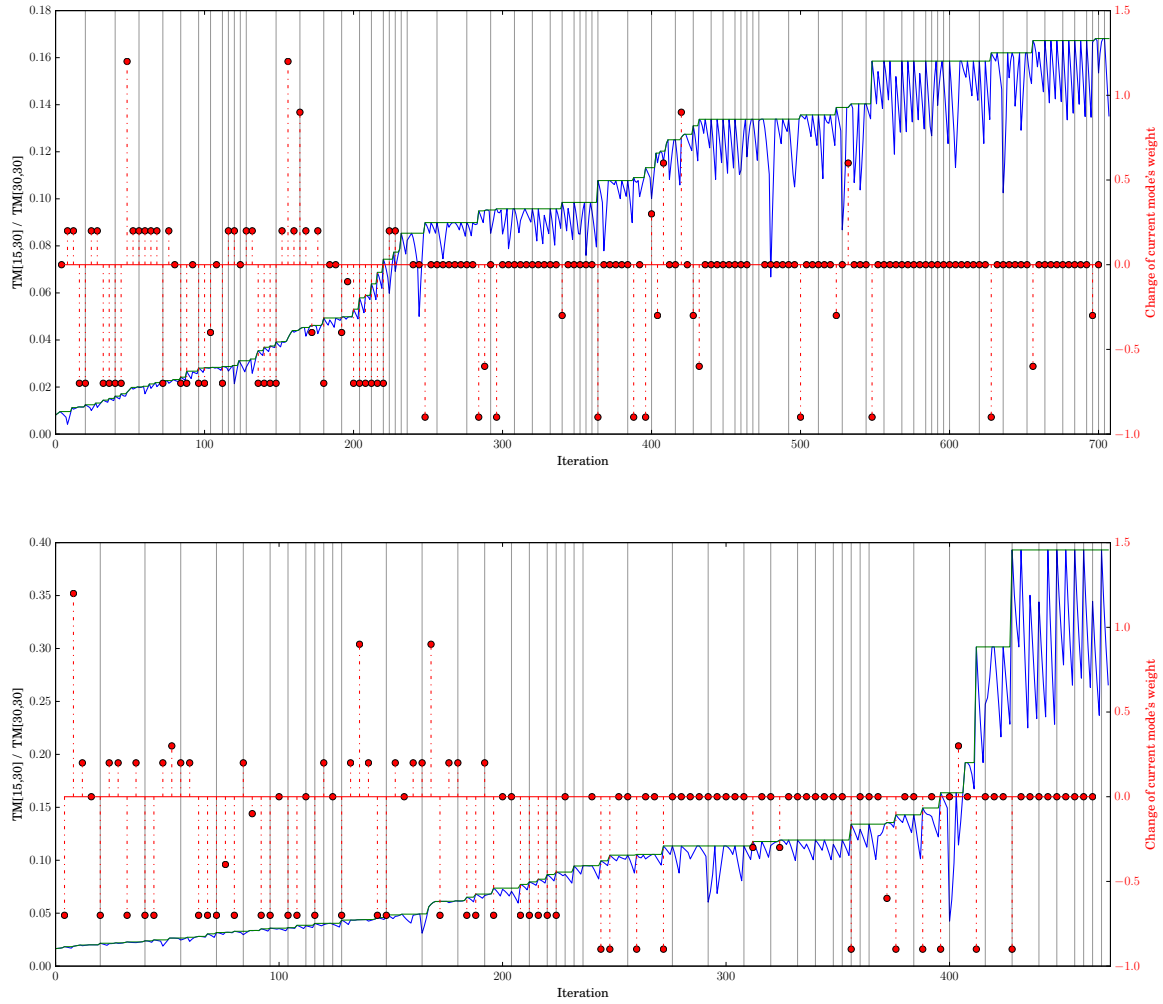


Figure A.1 – Two optimization results for maximizing target element TM[15,30]. The blue curve represents the value of the cost function at a given iteration. The green curve is the best result so far and the red handles represent the corresponding change of a mode's weight for a newly selected best pump configuration.

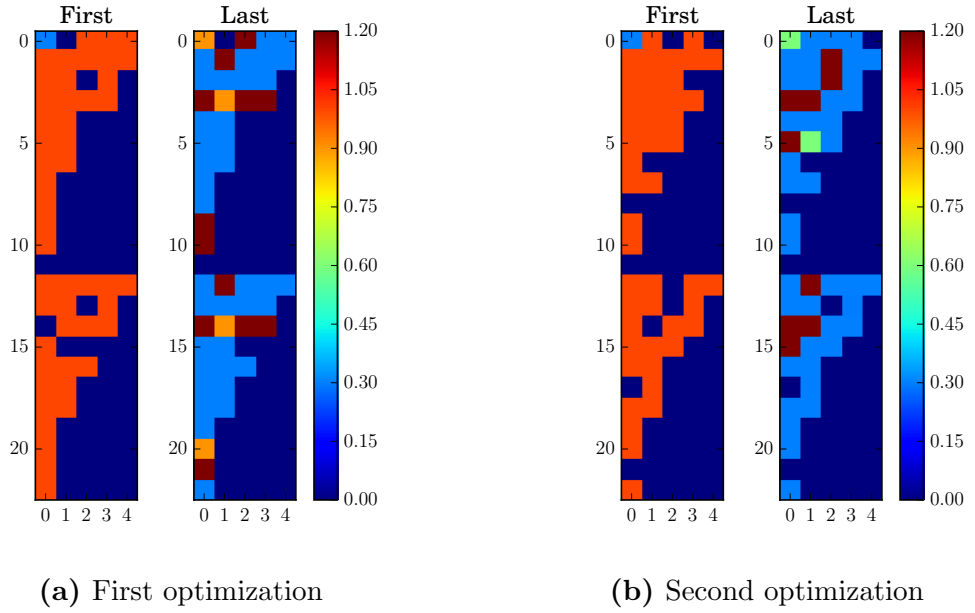


Figure A.2 – First and final pump configuration for the two optimization cases of Figure 3.1. The modes are indexed from 0 in both directions (LP_{01} becomes LP_{00}). Some randomly selected modes are turned off for each simulation.

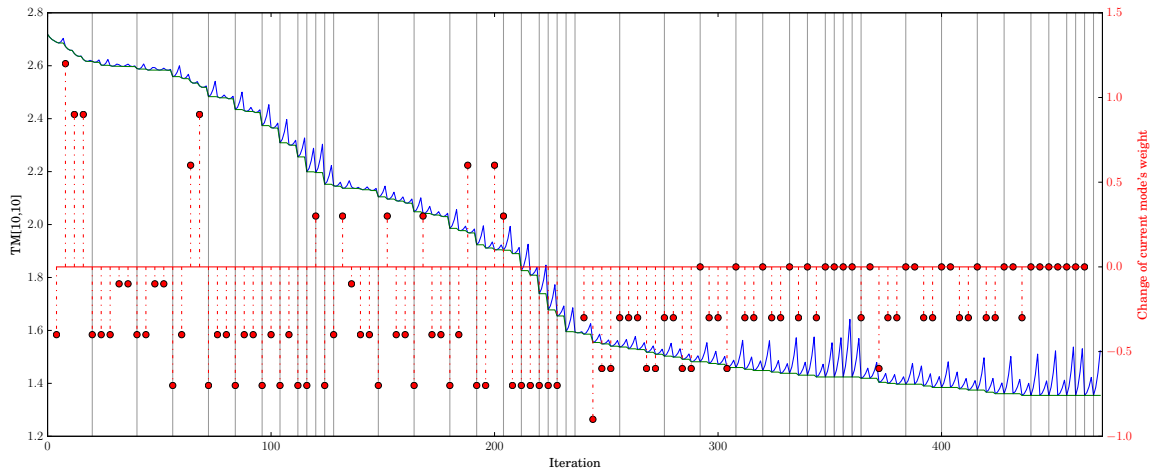


Figure A.3 – Optimization result for minimizing target element $TM[10, 10]$. The blue curve represents the value of the cost function at a given iteration. The green curve is the best result so far and the red handles represent the corresponding change of a mode's weight for a newly selected best pump configuration.

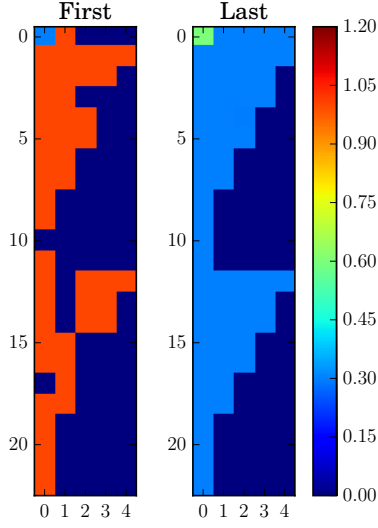


Figure A.4 – First and final pump configuration for the optimization of Figure A.3. The modes are indexed from 0 in both directions (LP_{01} becomes LP_{00}). Some randomly selected modes are turned off for each simulation.

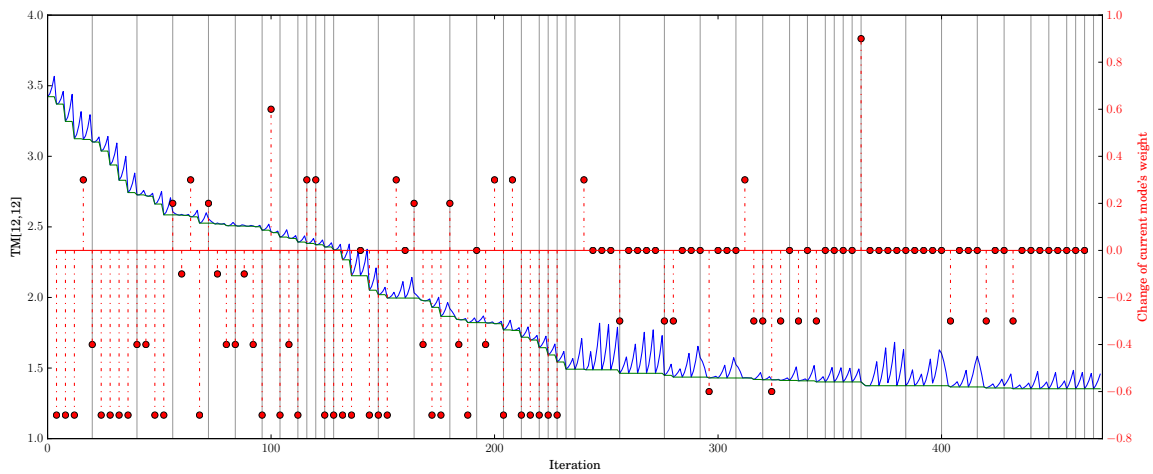


Figure A.5 – Optimization result for minimizing target element $TM[12, 12]$. The blue curve represents the value of the cost function at a given iteration. The green curve is the best result so far and the red handles represent the corresponding change of a mode's weight for a newly selected best pump configuration.

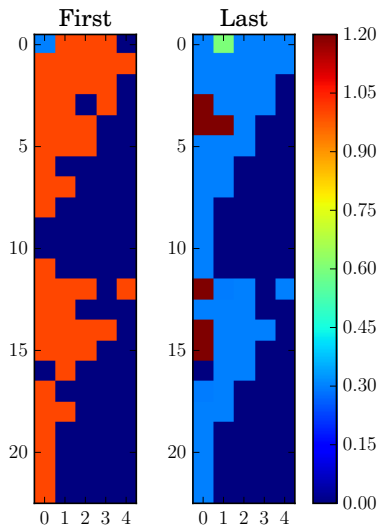


Figure A.6 – First and final pump configuration for the optimization of Figure A.5. The modes are indexed from 0 in both directions (LP_{01} becomes LP_{00}). Some randomly selected modes are turned off for each simulation.